RESEARCH ARTICLE

Design and construction of 3D printed devices to investigate active and passive bacterial dispersal on hydrated surfaces

Thierry Kuhn[1], Matteo Buffi[1], Saskia Bindschedler[1] , Patrick S. Chain[2] , Diego Gonzalez[1] , Claire E. Stanley[3] , Lukas Y. Wick[4] , Pilar Junier[1]* and Xiang-Yi Li Richter[1]*

Abstract

Background: To disperse in water-unsaturated environments, such as the soil, bacteria rely on the availability and structure of water films forming on biotic and abiotic surfaces, and, especially, along fungal mycelia. Dispersal along such "fungal highways" may be driven both by mycelial physical properties and by interactions between bacteria and fungi. However, we still do not have a way to disentangle the biotic and abiotic elements.

Results: We designed and 3D printed two devices establishing stable liquid films that support bacteria dispersal in the absence of biotic interactions. The thickness of the liquid film determined the presence of hydraulic flow capable of transporting non-motile cells. In the absence of flow, only motile cells can disperse in the presence of an energy source. Non-motile cells could not disperse autonomously without flow but dispersed as "hitchhikers" when co-inoculated with motile cells.

Conclusions: The 3D printed devices can be used as an abiotic control to study bacterial dispersal on hydrated surfaces, such as plant roots and fungal hyphae networks in the soil. By teasing apart the abiotic and biotic dimensions, these 3D printed devices will stimulate further research on microbial dispersal in soil and other water-unsaturated environments.

Keywords: 3D printing, Bacterial motility, Bacterial-fungal interactions, Fungal highways, Bacterial dispersal, Hitchhiking dispersal

Background

Spatial structure and physicochemical properties of microbial habitats strongly influence the composition and the ecological functions of microbial communities [1]. This is evident in water-unsaturated environments such as soils, where the combination of an unequal distribution of resources and the restricted movement of bacteria are often factors limiting their activity, as exemplified by the poor degradation of organic pollutants in soil ecosystems [2, 3]. Limited dispersal is particularly significant in the case of bacteria, as most types of active dispersal require liquid films at the interface of biotic and abiotic surfaces [4, 5]. Due to a lack of dispersal pathways in the form of continuous liquid films in water-unsaturated environments, the colonization and redistribution of bacteria to suitable habitats are restricted by their effective motility. In contrast to bacteria, dispersal limitation in water-unsaturated habitats is less of a problem for filamentous fungi [6]. Fungal mycelia extend readily in soils, colonizing also larger, air-filled pores that hinder bacterial dispersal most severely [7, 8]. Fungal mycelia can reach up to a total length of 10^2 m/g, 10^3 m/g, and

*Correspondence: pilar.junier@unine.ch; li@evolbio.mpg.de

[1] Institute of Biology, University of Neuchâtel, CH-2000 Neuchâtel, Switzerland
Full list of author information is available at the end of the article

10^4 m/g in arable, pasture, and forest soils, respectively [9, 10], providing a highly efficient and ubiquitous three-dimensional connective scaffold.

In recent years, several studies have shown that motile bacteria can utilize the continuous liquid films on the surface of likely hydrophilic and semi-hydrophobic hyphal networks to disperse, using so-called "fungal highways" [11–15]. Fungal networks are, however, not only a physical support resembling the highway system built by humans. Instead, hyphal networks continuously grow, reshape, and interact dynamically with the biotic and abiotic environment, including bacteria that disperse across them [16, 17]. The diverse interactions between bacteria and fungi on these fungal highways remain difficult to study, partly due to the intertwining roles of fungi as both providers of a dispersal network and active biological players. For instance, one important aspect of fungal highways is that it requires bacteria to actively disperse on the network. This may occur using one of the motility types described so far: swimming and swarming, which rely on extracellular filamentous appendages, or other forms of dispersal such as crawling, gliding, or twitching [18]. However, to date, the relative importance of these different motility types in navigating on the fungal highway is still unknown. Also, several mechanisms occurring as a result of or triggered by fungal highways dispersal could be better studied if the physical and biological properties of the dispersal network could be teased apart. This includes investigating the role of chemotaxis [19], cell-to-cell signaling [14, 19, 20], germination of dormant cells [21], gene transfer [22], or co-metabolism [3, 11, 12, 23], all of which have been observed in previous studies involving fungal highways. While glass fiber networks have been previously used to study such interactions [8, 12, 24], the rapid development of 3D printing technologies, including miniaturization, provides us with the opportunity to make customized devices to study the physical component of fungal networks. By studying bacterial dispersal on 3D printed models of fungal highways that provide a water film of defined properties (thickness, presence or absence of hydraulic flow), we can separate the part fungal mycelia play as a dispersal scaffold from the potential biotic interactions they exert on dispersing bacteria.

In this work, we designed two devices that reproduce a liquid-surface interface in the form of a meniscus, of varying thickness, as it may be found in hydrophilic soil surfaces or along fungal hyphae. The first device, which we term the "bacterial trail" can establish a relatively wide liquid film of 1.35 mm in lateral depth. The second device, which we term the "bacterial bridge" can establish much narrower liquid films of 0.14 mm in lateral depth. Motile bacterial cells dispersed in the liquid films

in both devices. Non-motile cells were unable to disperse alone in the liquid film on the bacterial bridge device, but they could disperse (probably as "hitchhikers" [14, 18, 25, 26]) in the presence of motile cells. Our devices lay a cornerstone for future investigations concerning microbial dispersal in natural unsaturated environments such as the soil and can be used to investigate the diverse and dynamic interactions between soil microorganisms occurring on fungal highways [18, 27]. They also serve as a proof of principle of the vast potential of applying 3D printing technologies to rapidly design, prototype, and produce customized tools in modern biology labs and their particular application in microbial ecology [28].

Results

Design and 3D printing of the devices

We designed two devices in an attempt to represent fungal hyphae under different water-saturation conditions. Printed parts can nowadays reach a resolution of 50 μm on the *x*- and *y*-axes and a resolution between 25 μm to 100 μm on the *z*-axis [29]; this is however still far from the real dimensions of a fungal hypha (typically hyphae are reported to have diameters on the order of 1–30 μm [30]). To replicate the liquid film formed by surface tension next to a hypha, we relied on a bar-shaped structure printed with a hydrophilic resin capable of maintaining a continuous liquid meniscus when connected to liquid reservoirs. In the first device, the "bacterial trail" (hereafter "trail" for brevity), the bar is placed on top of eight discrete liquid reservoirs (Fig. 1a); the "trail" device corresponds to wet conditions, where the liquid films forming on hydrophilic surfaces would be relatively thick (see below). The inoculation and end sampling wells were located directly below the bar along the longitudinal axis of the device. The other sampling wells (numbered from 1 to 6) were positioned to the sides of the bar, served to maintain a uniform thickness of the liquid film, and can also be used for sampling. In the liquid film on the "trail" device, small volume changes during inoculation or sampling can generate flow caused by pressure differences between the sampling wells, which may be able to transport non-motile particles such as bacterial cells and virus particles that do not have the ability to disperse actively. In the second device, the "bacterial bridge" (hereafter "bridge" for brevity), the bar mimicking fungal hyphae is placed at the top of two capillaries of 1 mm in diameter and 15 mm in height connected to two liquid reservoirs (interchangeable start and end sampling wells) (Fig. 1b); this device corresponds to water-limiting conditions where the liquid films are thinner and less susceptible to disturbance by volumetric changes in the reservoir, despite being continuous along the hydrophilic surface [31, 32]. In this way, the water film was also created and
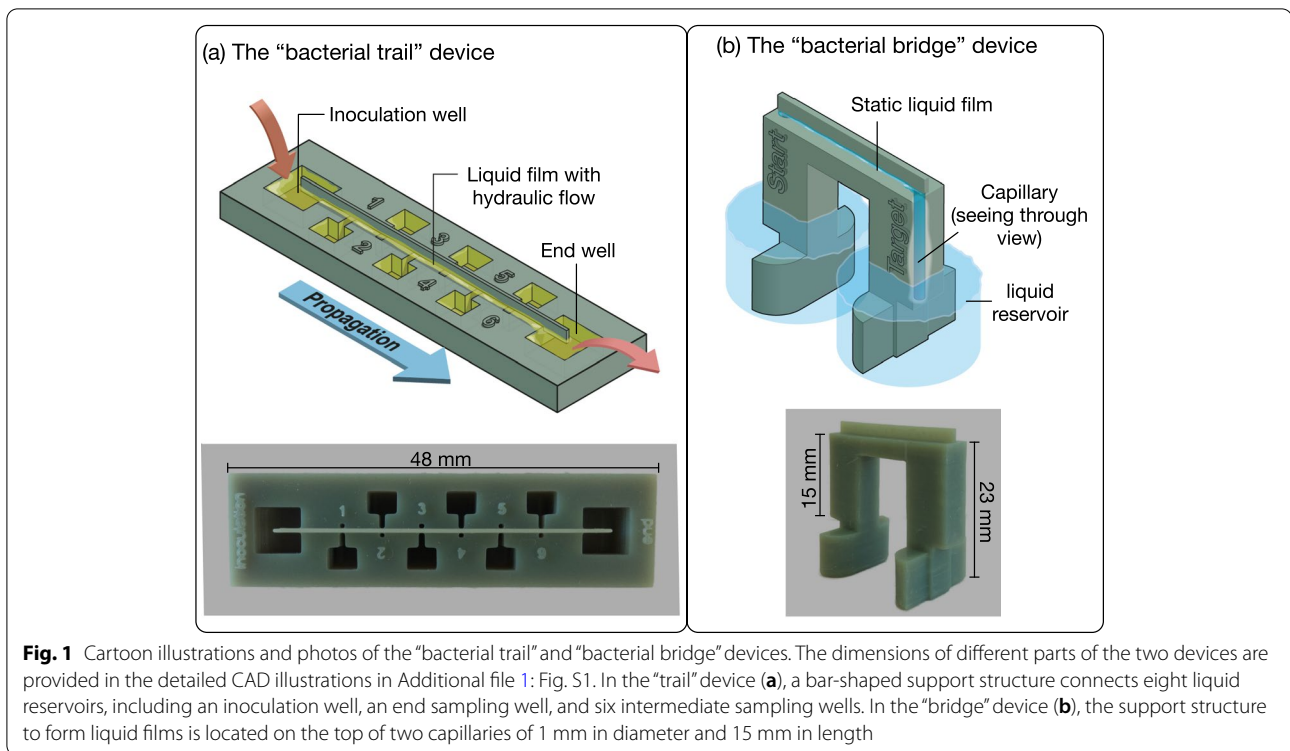
Fig. 1 Cartoon illustrations and photos of the "bacterial trail" and "bacterial bridge" devices. The dimensions of different parts of the two devices are provided in the detailed CAD illustrations in Additional file 1: Fig. S1. In the "trail" device (**a**), a bar-shaped support structure connects eight liquid reservoirs, including an inoculation well, an end sampling well, and six intermediate sampling wells. In the "bridge" device (**b**), the support structure to form liquid films is located on the top of two capillaries of 1 mm in diameter and 15 mm in length

maintained by surface tension, but in contrast to the "trail" device, sampling or changes in the volume of the liquid in the reservoirs did not generate flow. The dimensions of different parts of the two devices are provided in the detailed computer-aided design (CAD) illustrations in Additional file 1: Fig. S1. The two devices were 3D printed using a masked stereolithography (MSLA) printer. Corresponding Standard Tessellation Language—STL—files are provided in Additional files 2 and 3. The printing material has the desirable properties of being hydrophilic (with a contact angle of 52.8°, measured using a snake-based approach [33]), autoclavable, and biocompatible (Additional file 1: Table S1 and Fig. S2). Detailed printing and subsequent preparation procedures are provided in the Methods.

Characterization of the liquid films formed on the 3D printed devices

We generated liquid films on the "trail" and "bridge" devices (Fig. 2) following the procedures shown in the videos in Additional files 4 and 5 and described in the Methods. To control for the consistency of liquid film thickness (lateral depth), we measured the liquid films on four independently printed devices of each type at nine different locations on each device (Fig. 2, Box-Whisker charts). The liquid film lateral depth did not differ significantly between devices of the same type by pairwise Z-tests with a threshold p-value of 0.0083 (six pairwise comparisons for each device) adjusted using the Bonferroni correction (Additional file 1: Table S2). Across the "trail" devices, the liquid film had a lateral depth of 1.35 ± 0.32 mm ($n=4$). Across "bridge" devices, the liquid film had a lateral depth of 0.14 ± 0.04 mm ($n=4$), approximately one tenth of the liquid film lateral depth on the "trail" devices. The liquid film width on the "bridge" device can be adjusted by varying the length of liquid columns in the capillaries, which can be achieved by adding different volumes of liquid to the reservoirs (Additional file 1: Fig. S3). However, attention must be paid as the thinner the liquid film is, the more likely it will break during the duration of bacterial dispersal experiments if those last several days. The broader liquid film on the "trail" device allows flow caused by hydraulic pressure differences between the sampling wells. Using fluorescein as a marker, we measured the flow rate as the mean speed of marker transportation in the flow (1.19 mm/h, Additional file 1: Fig. S4, Additional files 6 and 7). In contrast, the narrower liquid films on the "bridge" device and the vertical capillaries connecting the liquid films to the sampling wells effectively suppressed flow caused by disturbances to the liquid in the sampling wells. We found that the traveling speed of fluorescein from the start well to the
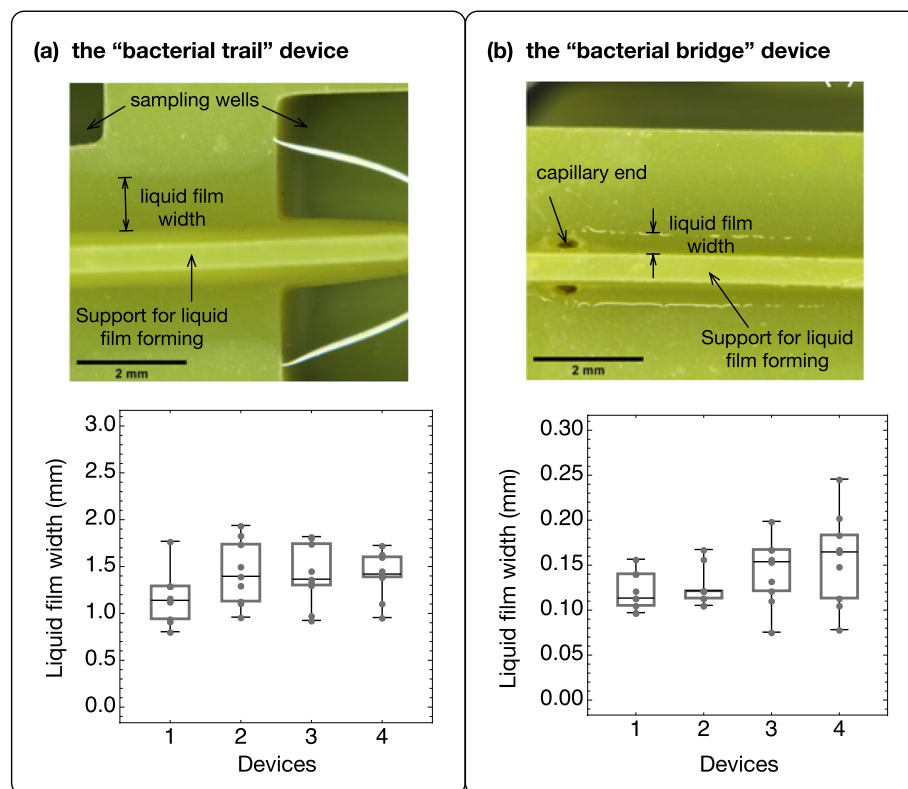
Fig. 2 Stereoscopic pictures of the liquid film on the "bacterial trail" (**a**) and "bacterial bridge" (**b**) devices and the distribution of the liquid film widths on four independently printed devices of each type. The photograph in each panel shows a typical stereoscopic image of the liquid films on the corresponding device. For each of the four devices of each type, a total of nine measurements of the liquid film width were measured and overlaid with the corresponding box-whisker chart. The middle line in each chart shows the median of the data points; the upper and lower boundaries of the boxes mark the 25% and 75% quantiles of the data. The liquid film widths do not differ significantly within a device type

end well can be explained by diffusion alone, suggesting the absence of hydraulic flow (Additional file 1: Fig. S4).

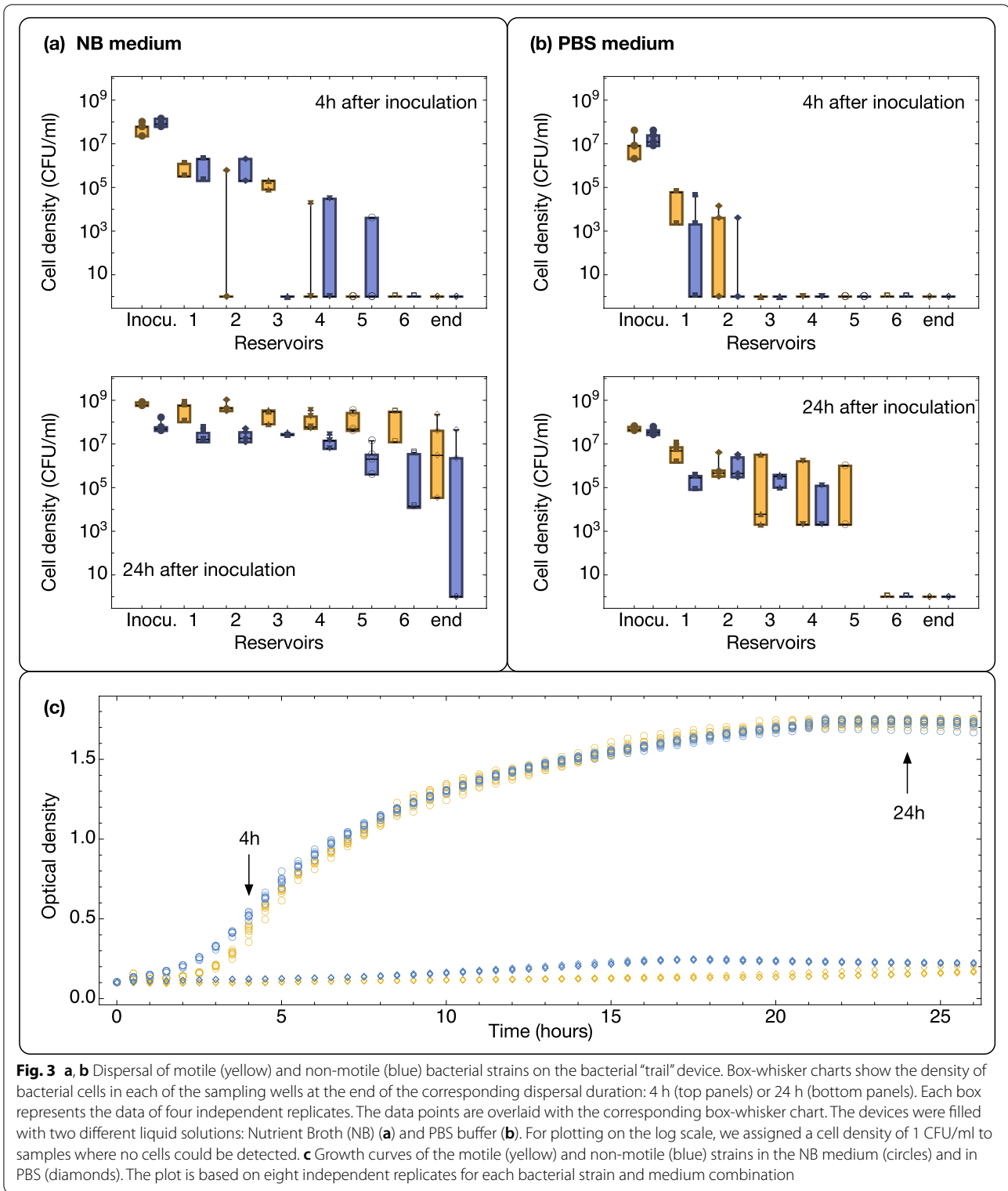### Active and passive dispersal in the liquid films on the two 3D printed devices

We used *Pseudomonas putida* KT2440 and its Δ*fliM* non-motile mutant strain to test the active and passive dispersal of cells in the liquid films on the "trail" and "bridge" devices.

Experiments with the "trail" device

Because of the presence of hydraulic flow in the liquid films on the "trail" device, we hypothesized that both strains could passively disperse from the inoculation well to other sampling wells driven by the flow. In addition, we expected the motile strains to have a dispersal advantage due to their ability to swim when sufficient energy sources are present in the environment. To test these hypotheses, we performed experiments under a full factorial design with the two bacterial strains (motile and non-motile), a culturing medium [nutrient broth (NB)

that contains the required nutrients for active dispersal and cell replication, and phosphate-buffered saline (PBS) solution, which does not contain any usable energy source], and two dispersal durations (4 h and 24 h), each with four replicates. At the start of the experiments, we inoculated 5 µl cell suspension (at an optical density of one) of either strain in the inoculation well. The cell density in each sampling well was quantified at the end of the corresponding dispersal duration (Fig. 3a, b). To establish the relative contribution of growth versus dispersal, we compared the growth curves of the two strains in NB and PBS (Fig. 3c).

For both dispersal durations, there was a general trend of decreasing cell densities at larger distances to the inoculation well. Robust two-way ANOVA tests showed that the density of cells differed significantly across sampling wells after 4 h ($p = 0.002$ for in NB and $p = 0.06$ in PBS) and after 24 h ($p < 0.001$ in NB and in PBS) of dispersal. The cell densities did not differ significantly between the motile and non-motile strains in either condition ($p = 0.299$ in NB and $p = 0.585$ in PBS) after 4 h of

Kuhn *et al. BMC Biology*   (2022) 20:203

Page 5 of 12

Fig. 3 **a**, **b** Dispersal of motile (yellow) and non-motile (blue) bacterial strains on the bacterial "trail" device. Box-whisker charts show the density of bacterial cells in each of the sampling wells at the end of the corresponding dispersal duration: 4 h (top panels) or 24 h (bottom panels). Each box represents the data of four independent replicates. The data points are overlaid with the corresponding box-whisker chart. The devices were filled with two different liquid solutions: Nutrient Broth (NB) (**a**) and PBS buffer (**b**). For plotting on the log scale, we assigned a cell density of 1 CFU/ml to samples where no cells could be detected. **c** Growth curves of the motile (yellow) and non-motile (blue) strains in the NB medium (circles) and in PBS (diamonds). The plot is based on eight independent replicates for each bacterial strain and medium combination

dispersal. After 24 h, the motile strain was significantly more abundant than the non-motile strain across sampling wells in NB ($p = 0.001$) but not in PBS ($p = 0.1$).

In the NB medium, the growth curves of the motile and non-motile strains differed significantly ($p < 0.001$) within the first 4 h of growth, with the non-motile strain

Kuhn *et al. BMC Biology*   (2022) 20:203

Page 6 of 12

growing significantly faster than the motile strain, but the overall growth did not differ significantly ($p = 0.3$) between the strains. In the PBS medium, both strains experienced minimal growth, with their optical densities barely doubled by 24 h, although the non-motile strain grew consistently more than the motile strain ($p < 0.001$).

Experiments with the "bridge" device

Because of the absence of hydraulic flow in the thin liquid film on the "bridge" device, we expected that only motile bacterial cells inoculated into the start well could disperse across the "bridge" and arrive at the target well. To test this hypothesis, we inoculated the motile and non-motile cells separately into the start well and tested the presence and density of cells in the target well after 72 h. Our pilot experiments showed that the motile strain already arrived at the target well within 20 h (data not shown), while the non-motile strain could not cross the "bridge" by diffusion in 72 h. The culturing medium contained nutrients (PBS+1% NB+1% Ficoll) to allow for energy-consuming bacterial swimming but sustained minimal growth and prevented the formation of a biofilm that could block the capillaries or help the non-motile strain to reach the target well through biofilm expansion (the growth curves of the two strains in the medium are provided in Additional file 1: Fig. S5). Our experiments showed that the motile cells arrived at the target well across all four replicates, while the non-motile cells did not arrive in all three replicates (Fig. 4a).

Non-motile bacteria are known to disperse along fungal hyphae by "hitchhiking" on motile bacterial cells [14]. To test whether this could happen in our system, we inoculated the motile and non-motile cells at a 1:1 ratio of cell numbers into the start well and tested the presence and cell densities of each cell type in the target well after 96 h. Both motile and non-motile cells were detected in the target well in five out of six replicates (Fig. 4b). In one replicate, the liquid film broke due to evaporation during the course of the experiments so that neither motile nor non-motile cells arrived at the target well (Fig. 4b, the failed replicate 5 is marked with an X). Because the motile and non-motile cells are tagged with green and red fluorescent proteins, respectively, we could distinguish them upon plating (Fig. 4c; corresponding color-blind-friendly pictures are provided in the Additional file 1: Fig. S4).

Discussion

3D printed devices as models to investigate bacterial dispersal

The dispersal capacity of bacteria in water unsaturated environments plays a crucial role in determining the spatial and temporal dynamics of microbial communities

and in turn their ecological functions [5]. In this work, we use 3D printing to produce two devices that generate continuous liquid films in which bacteria can disperse. The variable thickness of the films produced mimic typical liquid films formed on hydrophilic biological (i.e., plant roots or fungal hyphae [12, 14, 15, 34]) or abiotic surfaces. Thus, the devices can be used in control experiments involving bacterial dispersal on natural supports to help disentangle abiotic processes and biotic interactions. Due to the properties of the resin used, the devices have a hydrophilic surface for continuous liquid films to form, and are heat resistant up to 140 °C, enabling the devices to be autoclaved for sterilization and repeated use. The material cost for producing the devices is also low (0.35 USD per "bridge" device and 0.5 USD per "trail" device), allowing for affordability and widespread use.

The new experimental systems we developed allow for the study of bacterial dispersal under different water saturation conditions. Under some natural conditions, bacterial cells can be transported passively by flowing streams of water, such as percolation after rainfall or concentrated flow in cracks and macropores formed by growing plant roots in relatively dry soils [35, 36]. The relatively thick water films formed by the "trail" device serve to model this situation. By contrast, in unsaturated soils, bacterial dispersal is restricted by cell-substrate viscous drag and capillary pinning forces imposed by the thin and fragmented water films on the surface of substrates [31, 32]. In these cases, the pore water velocity drops below the movement speed of motile bacterial cells, and the effect of passive transportation (i.e., in hydraulic flow) on cell motion is then negligible [37]. The relatively thin and stationary water films formed by our "bridge" device capture this situation. A previous soil model showed that liquid films thicker than 5 μm were rare and rapidly drained even under mild suction conditions, and the resulting patchiness of the liquid films severely limits the dispersal capacity of bacteria [5]. Our results with the "bridge device" extended the conditions where non-motile bacteria cannot disperse alone in unsaturated soil. We showed that even in continuous water films (0.14 ± 0.04 mm on the "bridge" device) that were much broader than 5 μm, the non-motile cells were still unable to disperse unassisted (in the timeframe of the experiments, 72 h), although motile cells could efficiently disperse (over 2.1 cm). Similar results were found using glass fibers to represent fungal hyphae [12]. Although an estimation of the liquid film thickness on the mycelia of soil fungi under conditions corresponding to typical unsaturated soils is currently inexistent, we expect it to be thinner than the liquid films established with the bridge device. If this is the case, the widespread fungal highways may provide a dispersal advantage exclusive to flagellated bacteria and
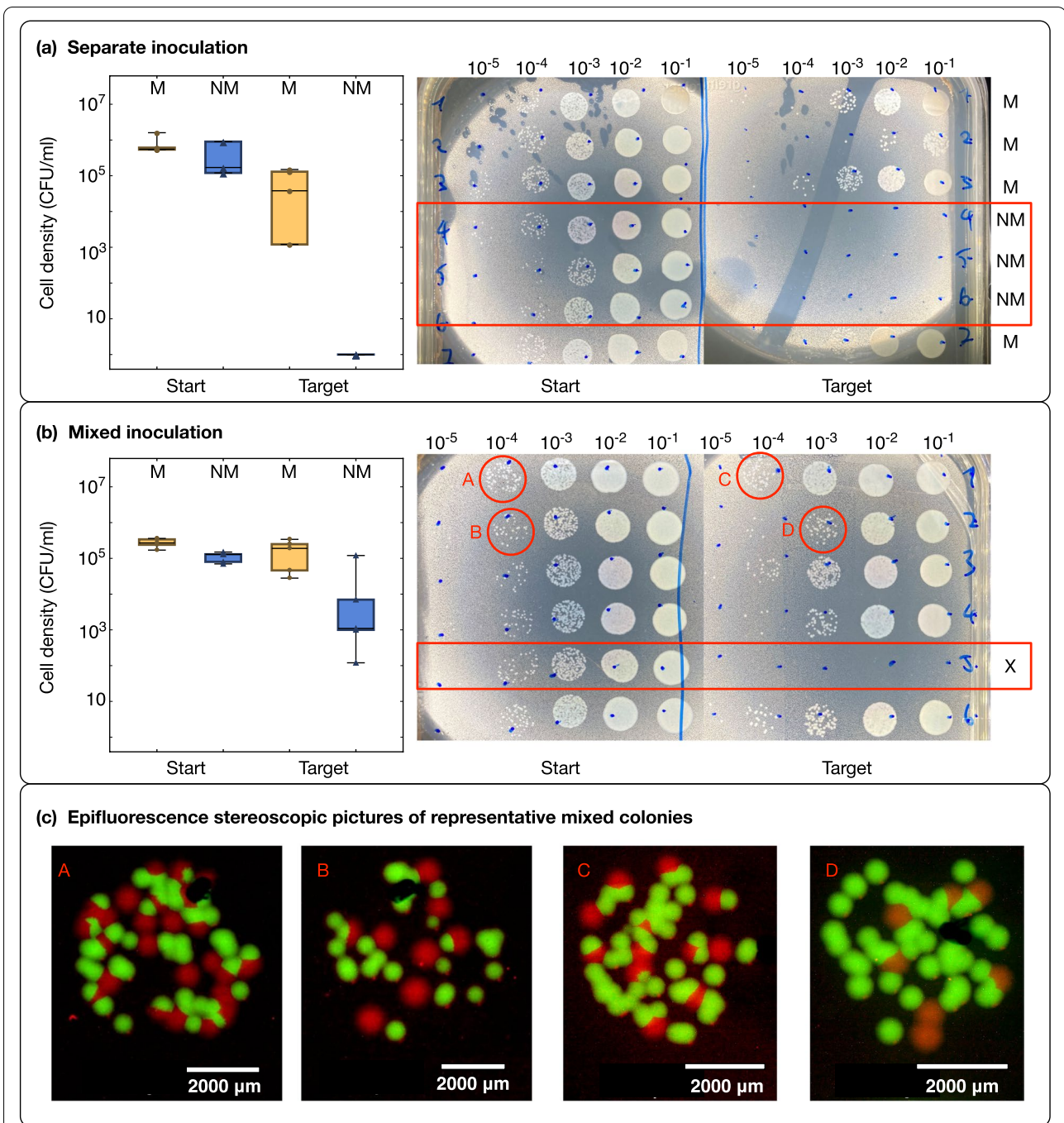
Fig. 4 Active dispersal of cells on the "bacterial bridge" device. **a** The box-whisker chart shows the cell densities of the motile (M) and non-motile (NM) bacterial cells in the start well and the target wells at 96 h after inoculation. The two bacterial strains were inoculated separately with four replicates for the M strain and three replicates for the NM strain. The two photographs show the dilution series performed to quantify cell densities in the start and target wells for each replicate. The corresponding dilution ratio is shown on top of each column (increasing level of dilution from right to left). Replicates 1, 2, 3, and 7 correspond to the motile strain; replicates 4, 5, and 6 correspond to the non-motile strain (marked with a red box in the image). **b** The box-whisker chart shows the same information as in **a** except that the two bacterial strains were mixed at a 1:1 ratio immediately before inoculation. The two photographs show the dilution series for quantifying cell densities in the start and target wells. Replicate five (marked with X) did not produce reliable results because the liquid film on top of the bacterial bridge broke during the experiment. **c** Epifluorescence stereoscopic micrographs of the mixed colonies in circles A to D are presented in the corresponding figures in the lower role of **b**

the non-motile bacteria that can hitchhike the dispersal of their associated carriers. This would be in accordance with the findings of a dispersal advantage of motile bacteria in cheese rind [38], and may contribute to explain the maintenance of costly flagella in soil bacteria [39].

Impact of liquid film lateral depth in dispersal of motile and non-motile cells

In the relatively thick liquid films established in the "trail" device (1.35 ± 0.32 mm in lateral depth), both motile and non-motile cells can disperse passively, driven by hydraulic flow. This explains why there was no significant difference in dispersal between motile and non-motile cells in the PBS solution across sampling wells (Fig. 3b). Because active dispersal by swimming with flagella requires energy [40, 41] and PBS lacks any carbon and energy sources, the motile cells can only disperse passively in a manner alike the non-motile cells. In the presence of energy sources, as in the NB medium, we expected the motile cells to have a dispersal advantage by being able to disperse actively by swimming, in addition to passive dispersal. Although the experimental results after 4 h did not support our hypothesis with statistical significance (probably due to stochastic effects on the distribution of cells within a short duration of time and the higher growth rate of the non-motile cells in the first hours after inoculation, which counterbalanced the dispersal advantage of the motile strain), the experimental results after 24 h provided clear evidence for a dispersal advantage of the motile cells over the non-motile cells, supporting our hypothesis.

In contrast to the relatively thick liquid films on the "trail" device, the liquid films on the "bridge" device are much thinner (0.14 ± 0.04 mm). The absence of hydraulic flow in these liquid films prevents non-motile cells from dispersal by drifting in the flow. This was shown in the single-strain inoculation experiments (Fig. 3a), which confirmed the importance of the flagellum for dispersal on hydrated surfaces such as in the case of fungal highways [34, 38, 39]. Interestingly, non-flagellated bacteria were still able to disperse in the presence of actively swimming motile cells, as shown in the co-inoculation experiments (Fig. 3b). Since the device does not introduce any biotic interaction between the dispersal network and the dispersing bacteria, we infer that the dispersal of non-motile bacteria facilitated by fungal highways [14, 20] may not require an active role of the fungus other than providing a continuous liquid pathway and a source of nutrients [21]. Although we do not know the exact mechanism explaining how the non-motile bacterial cells "hitchhike" to disperse in this particular case, existing literature provides some hypotheses that could be tested using our 3D printed devices. For instance, an

aspect that could be investigated in the future is whether physical attachment of the non-motile to the motile cells is required for transport or if the non-motile bacteria are dragged by the flow generated by motile bacteria. In previous studies, several non-motile bacterial species were found to attach to the cell body of the motile carrier bacterium *Capnocytophaga gingivalis* [42]; similarly, non-motile bacterial and fungal spores were found to attach to the flagella of their corresponding carriers [15, 25]. Based on these observations, different combinations of carriers and hitchhikers can be considered to test the possible release of chemicals to attract motile cells for attachment and dispersal [26], as well as the transport of non-motile cells as useful "cargo" to degrade antibiotics [43], or to invade an occupied niche [44]. These functional components of hitchhiking could be investigated in future experiments using our devices in combination with parallel experiments performed using fungal hyphae or other biological surfaces (e.g., plant roots).

Limitations and opportunities of 3D printed devices

Despite the advantages of the 3D printed devices (i.e., fast prototyping, low cost, and reusability), there are still technological limitations that are relevant to mention. The most important limitation is the relatively low printing resolution, which leads to roughness with staircase-like patterns on the printed surfaces that are not parallel or perpendicular to the printing bed. This limitation prevented us from generating a highly obtuse angle between support structures with smooth surfaces to reduce the thickness of the liquid film on the devices, which may be achievable by other (often more expensive) microfabrication technologies such as photolithography, which has been used in producing microfluidic devices. In the case of the "bridge" device, the liquid columns in the vertical capillaries suppress hydraulic flow that can transport non-motile cells [37]. In principle, the thinner the capillaries, the better the effect of suppressing flow. However, the printing resolution set a lower limit on the diameter of the capillaries (0.5 to 1 mm in our case). Because the capillaries are perpendicular to the plane where the liquid films form (and we need to prioritize the smoothness of printing on that surface), it was not possible to further reduce the diameter of the capillaries (e.g., by reorienting the devices on the printing bed). The limit on capillary diameter may have contributed to the breakage of the liquid film in one of the six replicates in the bacterial hitchhiking experiment (Fig. 4b). Despite this limitation, the bridge device is shown to be able to establish and maintain a thin water film of consistent width (Fig. 2b) for experiments over long durations (96 h in the hitchhiking dispersal experiments) with satisfying reliability. Moreover, the 3D printed devices offer the possibility of

Kuhn *et al. BMC Biology*   (2022) 20:203

Page 9 of 12

investigating the effect of two different boundaries (i.e., a surface-water and a water-air boundary) that complements other approaches such as microfluidic devices in which the water-air boundary is often not considered. In the last years, the cost of 3D printers has been decreasing rapidly to a few hundred USD. The expanding applications in the medical (especially dental) industry have promoted the development of a spectrum of hydrophilic biocompatible resins with diverse properties. In light of the increasing accessibility to 3D printing and affordable material costs, we view the two devices we developed in this work as early examples of much broader future applications of 3D printing in modern biology labs.

Conclusions

We designed and 3D printed two devices that can establish a thin liquid film to allow active or passive dispersal of bacteria, resembling the "fungal highway" mechanism of bacterial dispersal in the soil, but without introducing biotic interactions between the bacteria and fungi. By helping to tease apart the abiotic and biotic aspects of the interactions between bacteria and fungal mycelial networks, the devices we developed in this study open the door to many interesting future studies. For example, they can be used to identify and characterize fungi-secreted bioactive substances such as chemo-attractants, chemo-repellents, toxins, and signaling molecules. Furthermore, our work showcases the vast possibility and advantages of applying low-cost 3D printing technology to modern biology labs. We believe that the accessibility to fast prototyping and producing customized devices at affordable prices will play an increasingly important role in democratizing science and advancing education and research with more rational use of limited resources, such as in areas with disturbed production and supply chains.

Methods

3D printing and subsequent preparation of the devices

We designed the devices using the Autodesk Fusion 360 software, exported the design as STL files (provided in the Additional files 2 and 3), prepared the files for printing with the PrusaSlicer v2.2.0 software, and printed them using the HTR-140 green resin (3DM) with a masked stereolithographic 3D printer (Prusa SL1). The devices were printed directly on the printing bed with a layer height of 0.05 mm at 17 °C. The exposure time for each layer was 40 s for the first layer and 15 s for the rest layers. After printing, the devices were washed, blown with compressed air, and then dried overnight at room temperature. Finally, the devices were UV cured in a Prusa CW1 curing and washing machine for 4 min.

Building the liquid films on the devices and measuring their widths

To build a liquid film on the canal device, we first distributed 850 µl liquid (NB medium or PBS) in the eight sampling wells. Because of the hydrophilic property of the resin, water molecules can be attracted to the surface of the artificial hypha from the wells and spread along it automatically to form a liquid film. To make sure that the liquid film is continuous and is connected to each sampling well, we followed the artificial hyphae with the tip of a 1 ml pipette from one end to the other, going through all 8 wells. To build a liquid film on the bridge device, we first added 2.75 ml liquid each in two adjacent wells on a 24 well plate (Costar). We then placed the "start" and "target" ends of the bridge into the two wells. After that, we took 100 µl of liquid from the "start" well and ejected the liquid first at the openings of the two capillaries and then along the printed hypha. After a few seconds, most of the liquid flowed down along the two capillaries connecting the two sides of the "bridge" and the liquid surfaces in the two wells leveled off. The remaining liquid on top of the "bridge" device formed a continuous thin liquid film along the artificial hypha. Videos illustrating these procedures are provided in Additional files 4 and 5.

The widths of the liquid film on each of the devices were measured by taking pictures with a stereoscope (Nikon SMZ18) with a scale bar as reference. We measured the liquid films on four independently printed devices of each type and took three pictures at different locations (one in the middle and two in proximity to either end of the artificial hypha) on each device. We then measured the width of the liquid film at three randomly selected positions in each picture. This resulted in nine independent measurements of the liquid film width for each piece of the devices. The pictures were analyzed using the Fiji software (version 1.8.0). Using the burned-in scale as a reference, we could measure the width of the liquid film. For each picture, we performed three measurements at different randomly selected positions, leading to a total of nine independent measurements of the liquid film width for each piece of the devices.

Bacterial strains and the preparation for dispersal assays

We used an isogenic pair of motile and non-motile *P. putida* bacterial strains to test the active and passive transportation of cells in the liquid films formed on the devices. The motile KT2440 strain was isolated from the rhizosphere and is flagellated [45]. The non-motile strain is a non-flagellated (Δ*fliM*) mutant of the KT2440 strain, obtained by allelic exchange with a truncated version of *fliM* [31]. The motile strain is tagged with the green fluorescent protein, and the non-motile strain is tagged with

a red fluorescent protein (DsRed) marker. The two bacterial strains were cryo-preserved in 30% (v/v) glycerol at −80 °C. To reactivate the bacteria, cells were first plated on the Nutrient Agar (NA, 23 g/L, Carl Roth) through polygonal spreading and grown overnight at 30 °C in darkness. We then prepared bacterial suspensions from the overnight cultures by growing the cells in Nutrient Broth (NB, 23 g/L, Carl Roth) at ambient temperature under constant rotation at 120 rpm for 14 h. The bacterial suspension was adjusted with NB as blank to an optical density of 1 (600 nm wavelength), and centrifuged at 5000 g for 5 min to collect cells. The collected cells were washed once and resuspended in 0.01 M phosphate-buffered saline (PBS: 1.5 g/L $Na_2HPO_4 \cdot 2H_2O$, 0.25 g/L $NaH_2PO_4 \cdot 2H_2O$, 8.5 g/L NaCl) with 1% NB as an energy source. The cell suspension of each strain was adjusted to a final OD of 1.

Bacterial dispersal assays on the canal device

To test bacterial dispersal in the liquid film on the canal device, we performed experiments under a full factorial design with two different media (NB and PBS), two bacterial strains (motile and non-motile), and two dispersal durations (4 h and 24 h), each with 4 replicates. After building the liquid films with either NB or PBS, we added 10 μl of the cell suspension of either strain to the inoculation well. To maintain the liquid film and prevent evaporation during the experiments, we placed the devices into a large glass Petri dish with four pieces of sterile filter paper with 1 ml of autoclaved deionized water added to each. We took a sample of 20 μl from each of the eight wells following the order from one to eight at the end of each assay. The cell density in each of the wells was quantified (see below).

Bacterial dispersal assay on the bridge device

To test bacterial dispersal in the liquid film on the bridge device, we used a culture medium containing 0.01 M PBS with 1% of NB and 1% of Ficoll (10g/L, Sigma-Aldrich). We added Ficoll to the medium to increase its viscosity for suppressing flow [46]. As a thickening agent, Ficoll has the desirable properties of causing little osmotic stress and cannot be consumed or degraded by bacterial cells [47]. For the experiments, we first built liquid films on the devices and inoculated 5 μl of bacterial cell suspension (either the motile/non-motile strain alone or mixed with 1:1 ratio) to the start well. The devices were kept in a closed Petri dish to keep humidity high in darkness for 72 h for experiments where the inoculation contains only motile or non-motile cells. The experiments with inoculations that contain both motile and non-motile cells were run for 96 h under the same condition. At the end of the

experiments, we took a sample of 20 μl first from the target well and then from the start well of each device, and quantified the cell density in each sample.

Cell density quantification

We performed a dilution series to quantify the cell density in each sample taken at the end of the dispersal assays. Each of the 20 μl samples were diluted five times by adding 180 μl NB (10x dilution by volume). We then inoculated 5 μl of each of the five dilutions on a rectangular NA plate with a multichannel pipette. The plates were sealed with parafilm and incubated at 30 °C in darkness for 24 h. Afterwards, the lowest dilution that enabled counting of bacterial colonies formed by a single cell was chosen to determine the initial cell density in the corresponding sample.

Supplementary Information

The online version contains supplementary material available at https://doi.org/10.1186/s12915-022-01406-z.

Additional file 1: Fig. S1. Design details and photographs of the "bacterial trail" and "bacterial bridge" devices. **Fig. S2.** Growth curves of *P. putida* in Falcon tubes and the printed tubes. **Fig. S3.** Adjusting the liquid film width on the "bacterial bridge" device. **Fig. S4.** Transport of fluorescein in the liquid films on the devices. **Fig. S5.** Growth curves of the bacteria in different media. **Fig. S6.** Adjusted Fig. 4c for colorblind readers. **Table S1.** Biocompatibility control of the resin. **Table S2.** *p*-values of pairwise Z-tests of liquid film width.

Additional file 2. STL file of the "bacterial trail" device.

Additional file 3. STL file of the "bacterial bridge" device.

Additional file 4. Video of building the liquid film on the "bacterial trail" device.

Additional file 5. Video of building the liquid film on the "bacterial bridge" device.

Additional file 6. Video of fluorescein diffusion in the liquid film on the "bacterial trail" device.

Additional file 7. Video of fluorescein diffusion in the liquid film on the "bacterial bridge" device.

Authors' contributions
X-YLR and PJ designed the study, TK carried out the research, MB, SB, PSC, DG, CES, and LYW contributed to the research methods. X-YLR wrote the manuscript with inputs from all authors. All authors read and approved the final manuscript.

Availability of data and materials
The datasets supporting the conclusions of this article are included within the article and its additional files.

Kuhn *et al. BMC Biology*   (2022) 20:203

Page 11 of 12

Declarations

Ethics approval and consent to participate
Not applicable.

Consent for publication
Not applicable.

Competing interests
The authors declare that they have no competing interests.

Author details
[1]Institute of Biology, University of Neuchâtel, CH-2000 Neuchâtel, Switzerland. [2]Bioscience Division, Los Alamos National Laboratory, Los Alamos, NM 87545, USA. [3]Department of Bioengineering, Imperial College, South Kensington, London SW7 2AZ, UK. [4]Department of Environmental Microbiology, Helmholtz Centre for Environmental Research, 04318 Leipzig, Germany.

References

1. Andersson MGI, Berga M, Lindström ES, Langenheder S. The spatial structure of bacterial communities is influenced by historical environmental conditions. Ecology. 2014;95:1134–40.
2. Johnsen AR, Wick LY, Harms H. Principles of microbial PAH-degradation in soil. Environ Pollut. 2005;133:71–84.
3. Banitz T, Johst K, Wick LY, Schamfuß S, Harms H, Frank K. Highways versus pipelines: contributions of two fungal transport mechanisms to efficient bioremediation. Environ Microbiol Rep. 2013;5:211–8.
4. Tecon R, Or D. Biophysical processes supporting the diversity of microbial life in soil. FEMS Microbiol Rev. 2017;41:599–623.
5. Tecon R, Or D. Bacterial flagellar motility on hydrated rough surfaces controlled by aqueous film thickness and connectedness. Sci Rep. 2016;6:1–11.
6. Xiao X, Liang Y, Zhou S, Zhuang S, Sun B. Fungal community reveals less dispersal limitation and potentially more connected network than that of bacteria in bamboo forest soils. Mol Ecol. 2018;27:550–63.
7. Falconer RE, Houston AN, Otten W, Baveye PC. Emergent behavior of soil fungal dynamics: Influence of soil architecture and water distribution. Soil Sci. 2012;177:111–9.
8. Worrich A, König S, Miltner A, Banitz T, Centler F, Frank K, et al. Mycelium-like networks increase bacterial dispersal, growth, and biodegradation in a model ecosystem at various water potentials. Appl Environ Microbiol. 2016;82:2902–8.
9. Ritz K, Young IM. Interactions between soil structure and fungi. Mycologist. 2004;18:52–9.
10. Joergensen RG, Wichern F. Alive and kicking: why dormant soil microorganisms matter. Soil Biol Biochem. 2018;116:419–30.
11. Wick LY, Remer R, Würz B, Reichenbach J, Braun S, Schäfer F, et al. Effect of fungal hyphae on the access of bacteria to phenanthrene in soil. Environ Sci Technol. 2007;41:500–5.
12. Kohlmeier S, Smits THM, Ford RM, Keel C, Harms H, Wick LY. Taking the fungal highway: mobilization of pollutant-degrading bacteria by fungi. Environ Sci Technol. 2005;39:4640–6.
13. Bravo D, Cailleau G, Bindschedler S, Simon A, Job D, Verrecchia E, et al. Isolation of oxalotrophic bacteria able to disperse on fungal mycelium. FEMS Microbiol Lett. 2013;348:157–66.
14. Warmink JA, Nazir R, Corten B, van Elsas JD. Hitchhikers on the fungal highway: the helper effect for bacterial migration via fungal hyphae. Soil Biol Biochem. 2011;43:760–5.
15. Ingham CJ, Kalisman O, Finkelshtein A, Ben-Jacob E. Mutually facilitated dispersal between the nonmotile fungus *Aspergillus fumigatus* and the swarming bacterium *Paenibacillus vortex*. Proc Natl Acad Sci U S A. 2011;108:19731–6.
16. Deveau A, Bonito G, Uehling J, Paoletti M, Becker M, Bindschedler S, et al. Bacterial–fungal interactions: ecology, mechanisms and challenges. FEMS Microbiol Rev. 2018;42:335–52.
17. de Boer W. Upscaling of fungal–bacterial interactions: from the lab to the field. Curr Opin Microbiol. 2017;37:35–41.
18. Muok AR, Briegel A. Intermicrobial hitchhiking: how nonmotile microbes leverage communal motility. Trends Microbiol. 2021;29:542–50.
19. Furuno S, Päzolt K, Rabe C, Neu TR, Harms H, Wick LY. Fungal mycelia allow chemotactic dispersal of polycyclic aromatic hydrocarbon-degrading bacteria in water-unsaturated systems. Environ Microbiol. 2010;12:1391–8.
20. Warmink JA, van Elsas JD. Migratory response of soil bacteria to *Lyophyllum sp.* strain Karsten in soil microcosms. Appl Environ Microbiol. 2009;75:2820–30.
21. Worrich A, Stryhanyuk H, Musat N, König S, Banitz T, Centler F, et al. Mycelium-mediated transfer of water and nutrients stimulates bacterial activity in dry and oligotrophic environments. Nat Commun. 2017;8:1–9.
22. Berthold T, Centler F, Hübschmann T, Remer R, Thullner M, Harms H, et al. Mycelia as a focal point for horizontal gene transfer among soil bacteria. Sci Rep. 2016;6:36390.
23. Espinosa-Ortiz EJ, Rene ER, Gerlach R. Potential use of fungal-bacterial co-cultures for the removal of organic pollutants. Crit Rev Biotechnol. 2021;42:361–83.
24. Worrich A, König S, Banitz T, Centler F, Frank K, Thullner M, et al. Bacterial dispersal promotes biodegradation in heterogeneous systems exposed to osmotic stress. Front Microbiol. 2016;7:1214.
25. Muok AR, Claessen D, Briegel A. Microbial hitchhiking: how Streptomyces spores are transported by motile soil bacteria. ISME J. 2021;15:2591–600.
26. Hagai E, Dvora R, Havkin-Blank T, Zelinger E, Porat Z, Schulz S, et al. Surface-motility induction, attraction and hitchhiking between bacterial species promote dispersal on solid surfaces. ISME J. 2014;8:1147–51.
27. Yang P, van Elsas JD. Mechanisms and ecological implications of the movement of bacteria in soil. Appl Soil Ecol. 2018;129:112–20.
28. Nai C, Meyer V. From axenic to mixed cultures: technological advances accelerating a paradigm shift in microbiology. Trends Microbiol. 2018;26:538–54.
29. Gaikwad SR, Pawar NH, Sapkal SU. Comparative evaluation of 3D printed components for deviations in dimensional and geometrical features. Mater Today Proc. 2021. https://doi.org/10.1016/j.matpr.2021.11.157.
30. Islam MR, Tudryn G, Bucinell R, Schadler L, Picu RC. Morphology and mechanics of fungal mycelium. Sci Rep. 2017;7:13070.
31. Dechesne A, Wang G, Gülez G, Or D, Smets BF. Hydration-controlled bacterial motility and dispersal on surfaces. Proc Natl Acad Sci U S A. 2010;107:14369–72.
32. Wang G, Or D. Aqueous films limit bacterial cell motility and colony expansion on partially saturated rough surfaces. Environ Microbiol. 2010;12:1363–73.
33. Stalder AF, Kulik G, Sage D, Barbieri L, Hoffmann P. A snake-based approach to accurate determination of both contact points and contact angles. Colloids Surf A Physicochem Eng Asp. 2006;286:92–103.
34. Simon A, Bindschedler S, Job D, Wick LY, Filippidou S, Kooli WM, et al. Exploiting the fungal highway: development of a novel tool for the in situ isolation of bacteria migrating along fungal mycelium. FEMS Microbiol Ecol. 2015;91:fiv116.
35. Breitenbeck GA, Yang H, Dunigan EP. Water-facilitated dispersal of inoculant *Bradyrhizobium japonicum* in soils. Biol Fertil Soils. 1988;7:58–62.
36. Hekman WE, Heijnen CE, Burgers S, van Veen JA, van Elsas JD. Transport of bacterial inoculants through intact cores of two different soils as affected by water percolation and the presence of wheat plants. FEMS Microbiol Ecol. 1995;16:143–57.
37. Ebrahimi AN, Or D. Microbial dispersal in unsaturated porous media: characteristics of motile bacterial cell motions in unsaturated angular pore networks. Water Resour Res. 2014;50:7406–29.
38. Zhang Y, Kastman EK, Guasto JS, Wolfe BE. Fungal networks shape dynamics of bacterial dispersal and community assembly in cheese rind microbiomes. Nat Commun. 2018;9:336.
39. Pion M, Bshary R, Bindschedler S, Filippidou S, Wick LY, Job D, et al. Gains of bacterial flagellar motility in a fungal world. Appl Environ Microbiol. 2013;79:6862–7.
40. Schavemaker PE, Lynch M. Flagellar energy costs across the Tree of Life. BioRxiv 2022. https://doi.org/https://doi.org/10.1101/2022.01.31.478446.
41. Morowitz HJ. The energy requirements for bacterial motility. Science. 1979;1954(119):286.

42. Shrivastava A, Patel VK, Tang Y, Yost SC, Dewhirst FE, Berg HC. Cargo transport shapes the spatial organization of a microbial community. Proc Natl Acad Sci U S A. 2018;115:8633–8.

43. Finkelshtein A, Roth D, Ben Jacob E, Ingham CJ. Bacterial swarms recruit cargo bacteria to pave the way in toxic environments. MBio. 2015;6:e00074–15.

44. You X, Kallies R, Kühn I, Schmidt M, Harms H, Chatzinotas A, et al. Phage co-transport with hyphal-riding bacteria fuels bacterial invasion in a water-unsaturated microbial model system. ISME J. 2021. https://doi.org/10.1038/s41396-021-01155-x.

45. Regenhardt D, Heuer H, Heim S, Fernandez DU, Strömpl C, Moore ERB, et al. Pedigree and taxonomic credentials of Pseudomonas putida strain KT2440. Environ Microbiol. 2002;4:912–5.

46. Qu Z, Temel FZ, Henderikx R, Breuer KS. Changes in the flagellar bundling time account for variations in swimming behavior of flagellated bacteria in viscous media. Proc Natl Acad Sci U S A. 2018;115:1707–12.

47. Bremer E, Krämer R. Responses of microorganisms to osmotic stress. Annu Rev Microbiol. 2019;73:313–34.

Publisher's Note

Springer Nature remains neutral with regard to jurisdictional claims in published maps and institutional affiliations.